Electromagnetic Wave Propagation in Lossy Ferrites

FRED J. ROSENBAUM

Summary—The square of the complex transverse propagation constant in a lossy, magnetized ferrite is found to be described approximately by a circle in the complex plane when the magnetic field is varied. A graphical method for obtaining approximate values for the transverse propagation constant when the wave number in the direction of the applied field is given and real is derived here. This method is used to find the power absorbed from an incident plane wave by a semi-infinite ferrite as a function of the magnetizing field amplitude.

I. Introduction

THE PROBLEM of electromagnetic wave propagation in a magnetized lossy ferrite has been treated by Tannenwald and Seavey [1] for propagation along and normal to the direction of applied magnetic field with the assumption of a complex scalar permeability. The general case of plane waves propagating at an angle with respect to the magnetic field through a lossy anisotropic ferrite is treated here.

The propagation constant or wave number which describes plane wave propagation in a magnetized ferrite is a function of direction and is complex when the medium is lossy. The effect of loss is considered by including a damping term in the equation of motion of the microwave magnetization vector whose solution leads to an anisotropic permeability tensor with complex elements.[1] A digital computer is usually employed if numerical values of the propagation constant are sought because of the number of basic variables and the complex expression involved.

In the investigation of Cerenkov radiation in ferrites [2] such a computation was carried out. It is noted that a circle results when the square of the transverse propagation constant is plotted in the complex plane as a function of applied magnetic field for a given value of the loss parameter. When the magnetic field is fixed and the loss parameter is varied, the square of the transverse propagation constant again describes a circle which is orthogonal to the family of constant loss parameter circles. The two families of circles (constant magetic field, constant loss) form a pattern similar to that of a Smith Chart [3].

The approach taken to find analytic expressions for the circles observed numerically (for example see Fig. 13) is to seek a bilinear form for the complex variable equation relating the transverse propagation constant to the magnetizing field and the ferrite loss. It is shown that the resulting equation is not bilinear but becomes bilinear for certain approximations. Lines in the field-loss plane are transformed under these approximations into circles in the complex plane defined by the real and imaginary parts of the square of the transverse propagation constant. Although this result is only approximately correct, the approximation is good over a wide range of the ferrite parameters. Expressions for the centers of these circles and their radii are derived. This technique is used to find the power absorbed from a plane wave normally incident on a semi-infinite ferrite for the special case of transverse propagation.

The method described here may be used whenever the longitudinal wave number is given, for example in the case of Cerenkov radiation from an electron beam in a magnetized ferrite since the beam velocity determines the longitudinal wave number.

II. Notation

For a ferrite magnetized in the z direction the tensor permeability is [4]

$$\overline{^2\mu} = \mu_0 \begin{bmatrix} \mu & -j\kappa & 0 \\ j\kappa & \mu & 0 \\ 0 & 0 & 1 \end{bmatrix} \tag{1}$$

where

$$\mu = 1 + \frac{\omega_C \omega_M}{\omega_C^2 - \omega^2} \tag{2}$$

$$\kappa = \frac{\omega_M \omega}{\omega_C^2 - \omega^2} \tag{3}$$

and

ω = frequency of interest
$\omega_C = \omega_H + j\omega_R$
$\omega_H = \gamma H_i$ = precession frequency
$\omega_M = \gamma(4\pi M_s)$
$\omega_R = \alpha\omega = 1/T$
γ = gyromagnetic ratio (2.8×10^6 cps/oe)
H_i = internal dc magnetic field
$4\pi M_s$ = saturation magnetization of ferrite
T = macroscopic relaxation time which includes spin-spin and spin-lattice damping
μ_0 = permeability of free space.

As a result of the anistropy two characteristic plane waves exist in the ferrite for every direction of propagation. They are usually denoted as ordinary and extraordinary modes. These are described by two transverse propagation constants (ρ_1, ρ_2) which appear in the arguments of the functions which determine the radial behavior of fields in the ferrite.

Manuscript received April 6, 1964; revised June 16, 1964. The work described in this paper was initiated at the University of Illinois, Urbana, under the sponsorship of ASD, Wright-Patterson Air Force Base, Ohio, Contract No. AF 33(659)-10224, and completed under the sponsorship of McDonnell Aircraft Corp., St. Louis, Mo.
The author is with the Research Division, McDonnell Aircraft Corp., St. Louis, Mo. He was formerly with the University of Illinois, Urbana, Ill.

[1] See Appendix.

III. Mathematical Statement of Problem

The propagation of a plane wave in a lossy anisotropic ferrite may be described by a propagation vector $\bar{k}$

$$\bar{k} = \bar{\rho} + \bar{\zeta} \tag{4}$$

where $\bar{\zeta}$ is the component along the direction of magnetization and $\bar{\rho}$ is the component normal to this direction, as shown in Fig. 1 for a cylindrical coordinate system. The problem of finding $\bar{k}$ for the principal directions in a lossy plasma has been treated graphically by Weeks and Deschamps [5]. The problem of finding $\bar{k}$ as a function of direction in a lossless plasma is also described there. Here we are concerned with finding $\bar{\rho}$ and $\bar{k}$ if $\bar{\zeta}$ is known and real.

The equation which ρ and ζ satisfy may be derived from a knowledge of the microwave magnetic fields in the ferrite[2] and can be shown to be biquadratic in ρ, *i.e.*,

$$\mu\rho^4 - [(\mu^2 - \kappa^2 + \mu)k_0^2 - (1 + \mu)\zeta^2]\rho^2 + [\zeta^4 - 2\mu k_0^2\zeta^2 + k_0^4(\mu^2 - \kappa^2)] = 0 \tag{5}$$

where

$k_0^2 = (\omega/C)^2\epsilon_f$

ϵ_f = ferrite relative dielectric constant

C = speed of light in vacuum.

Eq. (5) may be expanded in terms of the ferrite parameters using (2) and (3) and grouped by descending powers of ω_C with the result

$$\omega_C^2(\rho^2 - \rho_0^2) + \omega_M\omega_C(\rho^2 - \rho_0^2)(\rho^2 - 2k_0^2) - \omega^2(\rho^2 - \rho_0^2)^2 + \omega_M^2k_0^2(k_0^2 - \rho^2) = 0 \tag{6}$$

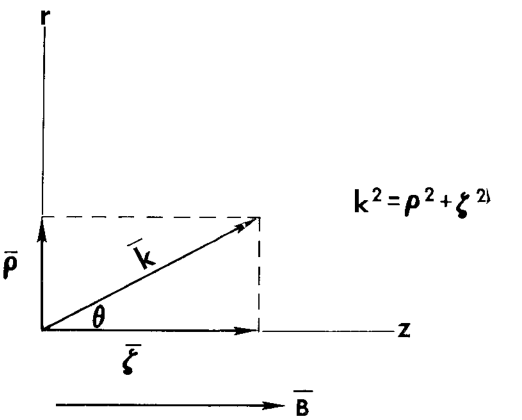

Fig. 1—Longitudinal and normal components of wave vector.

[2] Eq. (5), usually written in terms of the propagation number k, may be obtained by replacing $-\Gamma^2$ by $\rho^2+\zeta^2$ in Eq (7-6), p. 298 of Lax and Button [8]. It should also be pointed out that (5) is identical with the expression derived by Kales [9] for the transverse propagation constants if his γ^2 is replaced by $-\zeta^2$.

where

$$\rho_0^2 = k_0^2 - \zeta^2$$

i.e., that value of ρ which makes $k = k_0$ for a given ζ.

Eq. (6) relates the complex variable $\omega_C = \omega_M + j\omega_R$ to the complex variable ρ^2. The substitution $X = \rho^2 - \rho_0^2$, corresponding to a translation in the ρ^2 plane may now be made, giving

$$X^2[\omega_C^2 + \omega_M\omega_C - \omega^2] + X[\omega_M\omega_C(\rho_0^2 - 2k_0^2) - \omega_M^2k_0^2] + \omega_M^2k_0^2\zeta^2 = 0. \tag{7}$$

Since the observed circles all pass through the point $\rho^2 = \rho_0^2$, a transformation taking lines of constant ω_H and constant ω_R into circles in the ρ^2 plane must be obtained. Such a transformation is the inversion $X = 1/Y$. Inverting (7) and solving for Y gives

$$Y = \frac{\omega_C(2k_0^2 - \rho_0^2) + \omega_M k_0^2 \pm \sqrt{(\rho_0^2\omega_C + k_0^2\omega_M)^2 + 4\omega^2k_0^2\zeta^2}}{2\omega_M k_0^2\zeta^2}. \tag{8}$$

There will be two curves in the ρ^2 plane, corresponding to the choice of sign in (8), which represent the transformations of the ordinary and extraordinary modes. If these curves are to be circles, then the equation must represent a bilinear transformation of lines in the ω_C plane. If ζ is not a function of ω_C and $\zeta \neq 0$, (8) will be bilinear only if $\rho_0^2 = 0$, ($\zeta^2 = k_0^2$). It will be approximately bilinear if either term under the radical can be neglected.

Eq. (8) may be rewritten as

$$\frac{2\zeta^2}{\rho^2 - \rho_0^2} = 1 + \left[1 + \left(\frac{\zeta}{k_0}\right)^2\right]\frac{\omega_C}{\omega_M} \pm \sqrt{\left[1 + \left(\frac{\rho_0}{k_0}\right)^2\frac{\omega_C}{\omega_M}\right]^2 + \left[2\,\frac{\zeta}{k_0}\,\frac{\omega}{\omega_M}\right]^2}, \tag{9}$$

which reduces to the following in the limits of small and large ω_C/ω_M

$$\frac{\omega_C}{\omega_M} = 0$$

$$\rho^2 = \rho_0^2 + \frac{2\zeta^2}{1 \pm \sqrt{1 + \left[2\,\frac{\zeta}{k_0}\,\frac{\omega}{\omega_M}\right]^2}} \tag{10a}$$

and

$$\frac{\omega_H}{\omega_M} \to \infty \qquad \rho^2 = \rho_0^2. \tag{10b}$$

The curves of (8) go through the point $\rho^2=\rho_0^2$ for infinite applied field.

To neglect either term under the radical of (9) one of the following conditions must hold:

$$\text{a)}\quad \left|\omega_C+\frac{\omega_M}{\sin^2\theta_0}\right| \gg 2\omega\frac{\cos\theta_0}{\sin^2\theta_0}$$

$$\text{b)}\quad \left|\omega_C+\frac{\omega_M}{\sin^2\theta_0}\right| \ll 2\omega\frac{\cos\theta_0}{\sin^2\theta_0}.$$

The trigonometric identities are defined from Fig. 2. Fig. 3 shows the regions in the ω_C plane where a) and b) are satisfied, assuming that ρ_0^2 is real. The entire right half plane can satisfy condition a) if ω_M is sufficiently large. In most cases condition b) is of no interest since the precession frequency ω_H is assumed positive. If $2\omega\cos\theta_0/\sin^2\theta_0$ is sufficiently large, condition b) could be satisfied with some positive values of ω_H.

A binominal expansion for the radial of (8) may be used provided ω_C is chosen in the region of convergence. To a first approximation

$$\sqrt{(\rho_0^2\omega_C+k_0^2\omega_M)^2+4\omega^2k_0^2\zeta^2} \approx (\rho_0^2\omega_C+k_0^2\omega_M)+\frac{1}{2}\,\frac{4\omega^2k_0^2\zeta^2}{(\rho_0^2\omega_C+k_0^2\omega_M)}\cdot \quad (11)$$

It is important to note that for many values of ω_H (11) is a poor approximation. It improves, however, as $|\omega_C|$ increases.

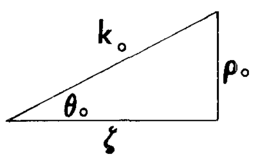

Fig. 2—Isotropic propagation constants.

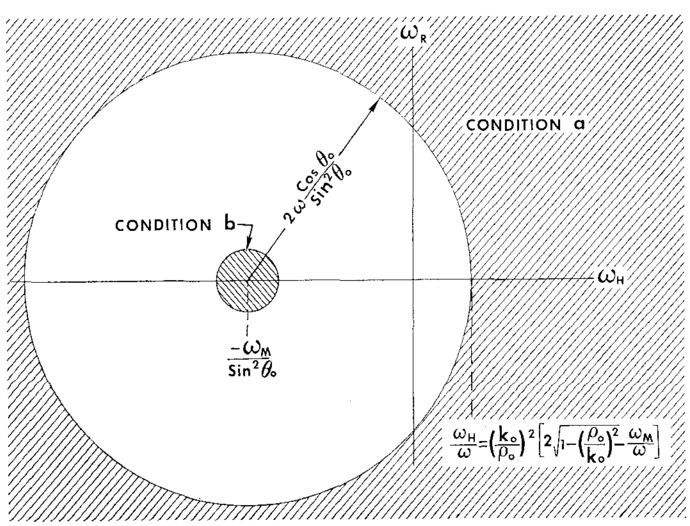

Fig. 3—Regions of the ω_C plane where approximately bilinear form is obtained.

Over the range of parameters where (11) is valid, the transformation Y now becomes

$$Y \approx \left\{\frac{\omega_C(2k_0^2-\rho_0^2)+\omega_Mk_0^2 \pm (\rho_0^2\omega_C+k_0^2\omega_M)}{2\omega_Mk_0^2\zeta^2} \pm \frac{\omega^2}{(\rho_0^2\omega_C+k_0^2\omega_M)}\right\}. \quad (12)$$

IV. The Inverse Transformation—Minus Root

The choice of the negative sign in (12) yields

$$Y_- \approx \frac{\omega_C}{\omega_Mk_0^2}-\frac{\omega^2}{\omega_M(\rho_0^2\omega_C+k_0^2\omega_M)} \quad (13)$$

with real and imaginary parts

$$u=\frac{1}{\omega_M}\left[\frac{\omega_H}{k_0^2}-\frac{\omega^2(\rho_0^2\omega_H+k_0^2\omega_M)}{(\rho_0^2\omega_H+k_0^2\omega_M)^2+(\omega_R\rho_0^2)^2}\right] \quad (14a)$$

$$v=\frac{\omega_R}{\omega_M}\left[\frac{1}{k_0^2}+\frac{(\omega\rho_0)^2}{(\rho_0^2\omega_H+k_0^2\omega_M)^2+(\omega_R\rho_0^2)^2}\right]. \quad (14b)$$

Points in the $\omega_C=\omega_H+j\omega_R$ plane which are easily mapped into the Y_- plane are shown in Table I. The transformation Y_- is the form $(az+b)+(1/cz+d)$ and is conformal. Lines of constant ω_H and constant ω_R in the ω_C plane are distorted in the Y_- plane as shown in Figs. 4(a) and 4(b). For practical ferrites at microwave frequencies, $0<(\omega_R/\omega)<0.1$, [6] and the region of interest in the ω_C plane is a narrow strip in the upper half of the right half plane.

With the assumption of reasonably low loss ferrites $(\omega_R/\omega)^2\approx 0$,[3] the line $\omega_H=$constant may be approximated in the Y_- plane by the line

$$u=\frac{1}{\omega_M}\left[\frac{\omega_H}{k_0^2}-\frac{\omega^2}{(\rho_0^2\omega_H+k_0^2\omega_M)}\right] \quad (15a)$$

while the line $\omega_R=$constant is represented by

$$v=\frac{\omega_R}{\omega_M}\left[\frac{1}{k_0^2}+\left(\frac{\omega\rho_0}{\omega_Mk_0^2}\right)^2\right] \quad (15b)$$

for ω_H/ω small as seen in Figs. 4(a) and 4(b). Thus the curves of these two figures have been approximated by the two straight lines of (15a) and (15b).

The inversion

$$X=\frac{1}{Y}$$

$$\gamma+j\delta=\frac{1}{u+jv}$$

[3] See Appendix.

TABLE I
POINTS IN THE Y-PLANE

ω_H	ω_R	u	v
0	0	$-\left(\frac{\omega}{\omega_M k_0}\right)^2$	0
Const.	0	$\frac{1}{\omega_M}\left[\frac{\omega_H}{k_0^2} - \frac{\omega^2}{\rho_0^2\omega_H + k_0^2\omega_M}\right]$	0
Const.	$\rightarrow\pm\infty$	$\frac{\omega_H}{\omega_M k_0^2}$	$\rightarrow\pm\infty$
0	Const.	$-\frac{\omega^2 k_0^2}{(\omega_M k_0^2)^2 + (\rho_0^2\omega_R)^2}$	$\frac{\omega_R}{\omega_M}\left[\frac{1}{k_0^2} + \frac{\omega^2\rho_0^2}{(\omega_M k_0^2)^2 + (\rho_0^2\omega_R)^2}\right]$
$\rightarrow\pm\infty$	Const.	$\rightarrow\pm\infty$	$\frac{\omega_R}{\omega_M k_0^2}$

carries these lines into circles in the X plane such that the line u = constant becomes the circle

$$\left(\gamma - \frac{1}{2u}\right)^2 + \delta^2 = \left|\frac{1}{2u}\right|^2 \tag{16a}$$

which is tangent to the imaginary axis, centered at $(1/2u, 0)$ and has radius $|1/2u|$ [7]. The line of constant v transforms into the circle

$$\gamma^2 + \left(\delta^2 + \frac{1}{2v}\right) = \left|\frac{1}{2v}\right|^2 \tag{16b}$$

which is tangent to the real axis with center $[0, -(1/2v)]$ and has radius $|1/2v|$. These are shown in Fig. 5 (page 522). Using (15a) and (15b) one obtains

$$\frac{1}{2u} = \frac{\omega_M k_0^2}{2}\left[\frac{(\rho_0^2\omega_H + k_0^2\omega_M)}{\omega_H(\omega_H\rho_0^2 + k_0^2\omega_M) - \omega^2 k_0^2}\right] \tag{17a}$$

$$\frac{1}{2v} = \frac{\omega_M k_0^2}{2\omega_R}\left[\frac{(\omega_M k_0)^2}{(\omega_M k_0)^2 + (\rho_0\omega)^2}\right]. \tag{17b}$$

For a specific ferrite the value of the loss parameter ω_R/ω, tabulated in [6], determines $1/2v$ independent of the applied magnetic field. A "constant loss" circle may now be drawn. For each value of ω_H/ω a "constant field" circle is generated. As ω_H/ω increases, the centers move along the negative real line toward negative infinity while the radii increase. As seen from (17a) when $\omega_H(\rho_0^2\omega_H + k_0^2\omega_M) = \omega^2 k_0^2$ the circle is centered at infinity and has infinite radius. For larger ω_H/ω the centers return along the positive real line while the radii decrease. The intersections of these circles with the "constant loss" circle generate the circular locus in the X plane.

Numerical evaluation of (17a) and (17b) yield a circular locus about 30 per cent smaller than that computed exactly (shown in the Appendix). Better results are obtained by including another term in the binominal expansion and by improving the approximation for the constant v line.

An average value for v may be defined as

$$\bar{v} = \frac{v_1 + v_2}{2}$$

where v_1 and v_2 are computed for two values of ω_H/ω. These values are chosen such that most of the circle has been traversed between them. For example, in the curves of the Appendix the points $\omega_{H_1}/\omega = 0.1$ and $\omega_{H_2}/\omega = 1.0$ yield a good approximation. Eqs. (17a) and (17b) could also have been used to establish these values.

Using the first three terms in the binomial expansion, an average v and the approximation $(\omega_R/\omega)^2 \approx 0$ one obtains

$$u = \frac{1}{\omega_M}\left[\frac{\omega_H}{k_0^2} - \frac{\omega^2}{(\rho_0^2\omega_H + k_0^2\omega_M)} + \frac{(\omega^2 k_0\zeta)^2}{(\rho_0^2\omega_H + k_0^2\omega_M)^3}\right] \tag{18a}$$

$$\bar{v} = \frac{\omega_R}{2\omega_M k_0^2}\left\{2 + \left(\frac{\omega\rho_0 k_0}{\rho_0^2\omega_{H_1} + k_0^2\omega_M}\right)^2 \cdot\left[1 - 3\left(\frac{\omega k_0\zeta}{\rho_0^2\omega_{H_1} + k_0^2\omega_M}\right)^2\right] + \left(\frac{\omega\rho_0 k_0}{\rho_0^2\omega_{H_1} + k_0^2\omega_M}\right)^2 \cdot\left[1 - 3\left(\frac{\omega k_0\zeta}{\rho_0^2\omega_{H_2} + k_0^2\omega_M}\right)^2\right]\right\}. \tag{18b}$$

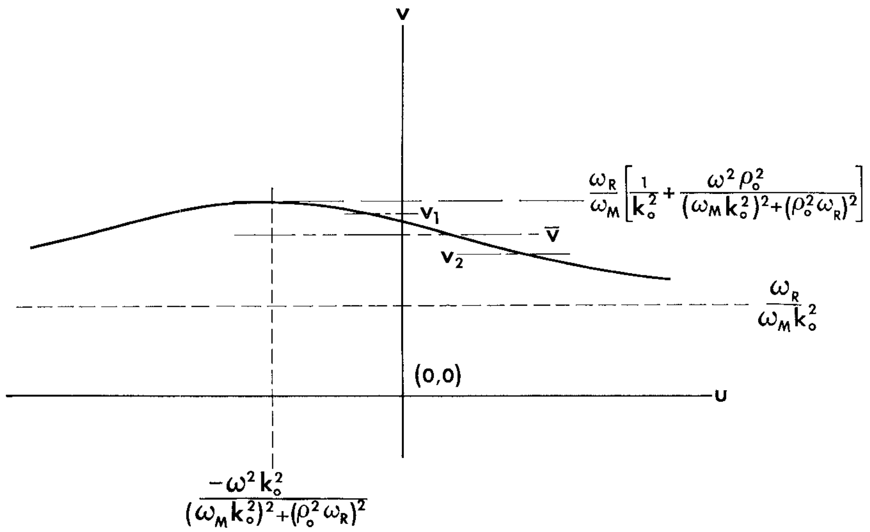

(a)

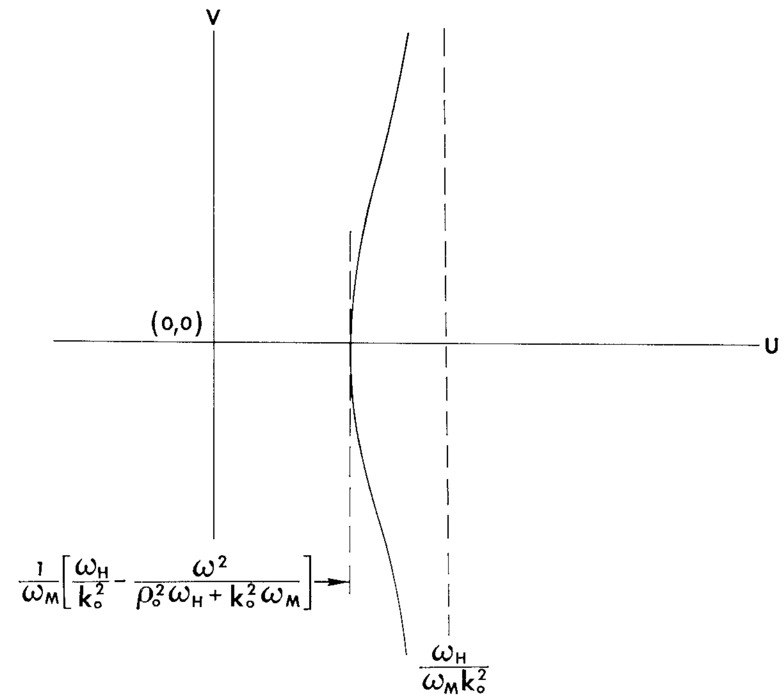

(b)

Fig. 4—(a) Mapping of ω_R=constant in the Y_- plane. (b) Mapping of ω_H=constant in the Y_- plane.

No average is necessary for u since in practical ferrites ω_R/ω is small so only values near $v=0$ are important.[4]

The circles defined by (18a) and (18b) are in the $X=\rho^2-\rho_0^2$ plane. To enter the ρ^2 plane a translation by ρ_0^2 is required. Representative circles in the ρ^2 plane, assuming ρ_0^2 real, are shown in Fig. 6. The intersection of a constant ω_H/ω circle with the constant ω_R/ω circle is the point $\rho^2(\omega_H/\omega, \omega_R/\omega)$.

Notice that the variables ω_H and ω_R and the constant ω_M can be normalized by ω to provide dimensionless quantities useful for computational purposes and which yield universal results.

To compare the accuracy of this approximate method with the exact computer results (shown in the Appendix) the following parameters were chosen.

$$\frac{\omega_{H_1}}{\omega} = 0.1 \qquad \frac{\omega_M}{\omega} = 1.0 \qquad \epsilon_f = 13$$

$$\frac{\omega_{H_2}}{\omega} = 1.0 \qquad \frac{\omega_R}{\omega} = 0.0192^{5} \qquad \zeta^2 = \left(\frac{\omega}{c}\right)^2 \quad (1.07)^2$$

The comparison is shown in Table II.

[4] See Fig. 4(a).

[5] Value for Ferramic R1 as determined by Sensiper [6].

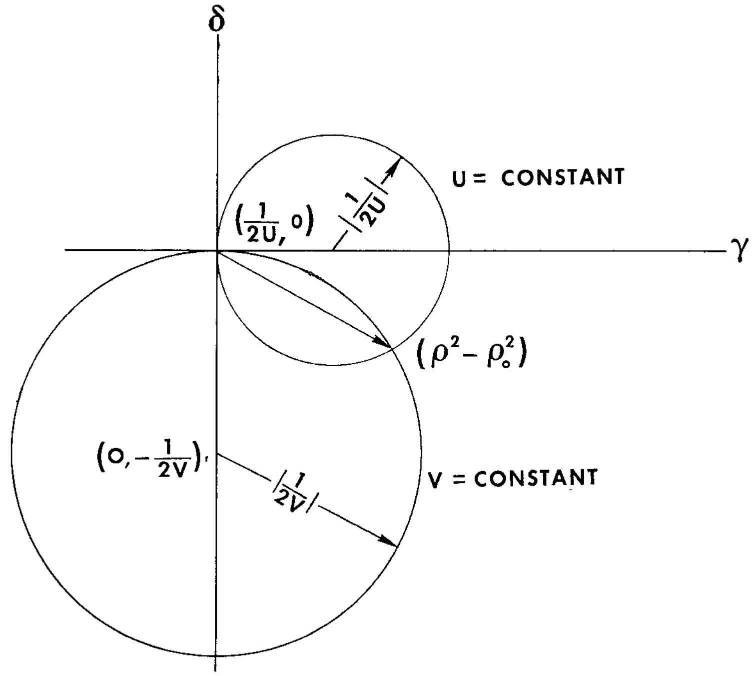

Fig. 5—Lines of constant u and v in the X_+ plane.

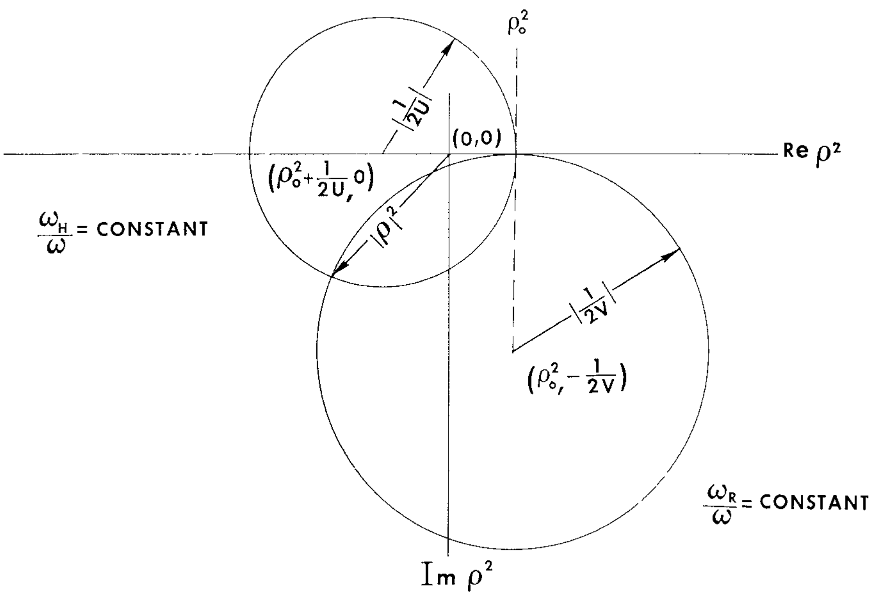

Fig. 6—Lines of constant ω_H/ω and ω_R/ω in the ρ^2 plane.

TABLE II

COMPARISON BETWEEN APPROXIMATE AND EXACT RESULTS

	Approximate Center	Exact Center
$\omega_H/\omega=0.59$	$-6534+j0$	$-6200+j0$
$\omega_R/\omega=0.0192$	$468-j9470$	$468-j10^4$
$\overline{\rho^2}=(\rho\lambda)^2$	$-8600-j6700$	$-8825-j6438$
	$=10,880/\underline{217.9°}$	$=10,900/\underline{216.1°}$

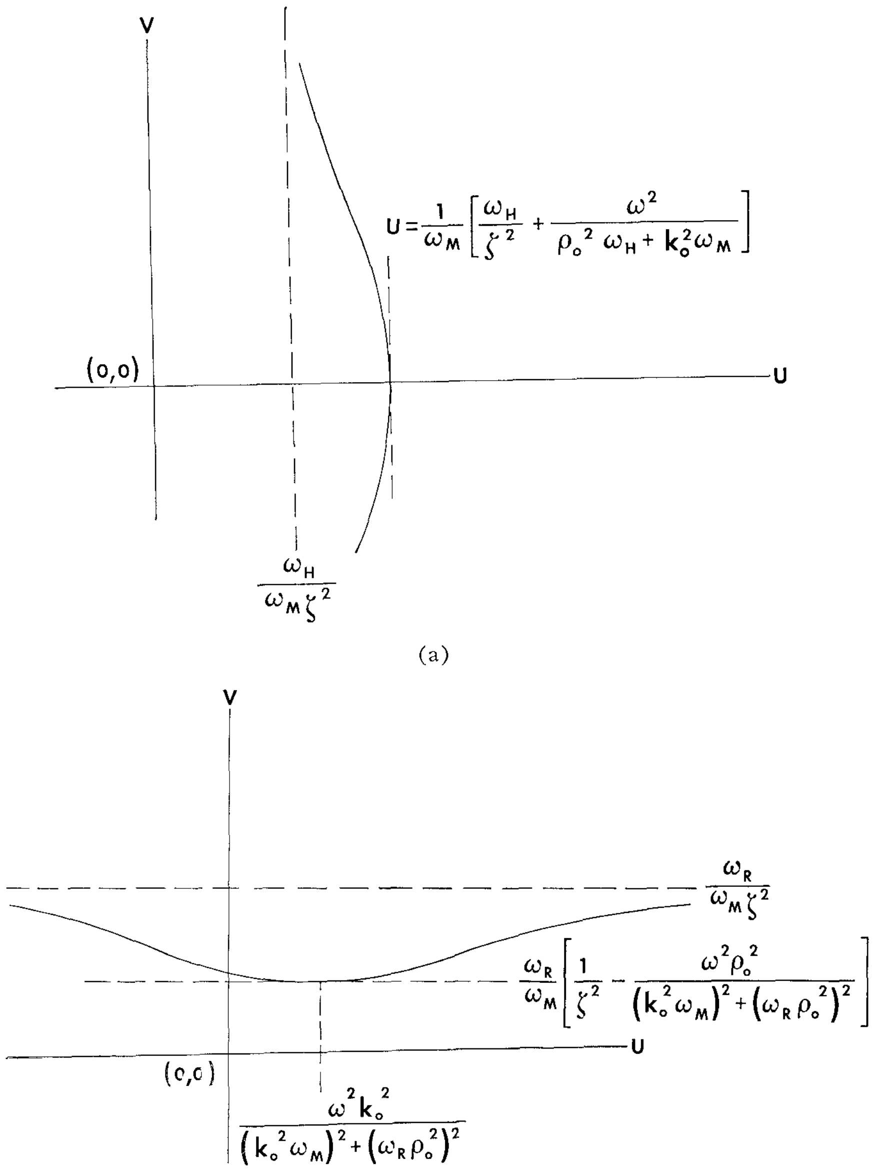

(b)

Fig. 7—(a) Mapping of ω_H=constant in the Y_+ plane. (b) Mapping of ω_R=constant in the Y_+ plane.

To use the inverse transformation one must:

1) Determine the behavior of constant ω_H and ω_R lines in the Y plane [Figs. 4(a) and 4(b)],
2) Approximate these curves by appropriate straight lines [Eqs. (18a) and (18b)],
3) Invert these approximate lines to obtain the circles in the X plane [Eqs. (16a) and (16b)],
4) Translate by ρ_0^2 to enter the ρ^2 plane.

THE INVERSE TRANSFORMATION—PLUS ROOT

The choice of the positive sign in (12) produces

$$Y_+ \approx \frac{\omega_C}{\omega_M\zeta^2} + \frac{\omega^2}{\omega_M(\rho_0^2\omega_C + k_0^2\omega_M)} \tag{19}$$

with real and imaginary parts

$$u = \frac{1}{\omega_M}\left[\frac{\omega_H}{\zeta^2} + \frac{\omega^2(\rho_0^2\omega_H + k_0^2\omega_M)}{(\rho_0^2\omega_H + k_0^2\omega_M)^2 + (\omega_R\rho_0^2)^2}\right] \tag{20a}$$

$$v = \frac{\omega_R}{\omega_M}\left[\frac{1}{\zeta^2} - \frac{(\omega\rho_0)^2}{(\rho_0^2\omega_H + k_0^2\omega_M)^2 + (\omega_R\rho_0^2)^2}\right]. \tag{20b}$$

A line of constant ω_H transforms into the curve of Fig. 7(a) while a constant ω_R line is shown in Fig. 7(b). The origin (ω_M, $\omega_R = 0$) is translated to

$$u = \frac{1}{k_0^2}\left(\frac{\omega}{\omega_M}\right)^2$$

$$v = 0.$$

Notice that for Y_+ the origin is located at $u > 0$ while for Y_- it is at $u < 0$.

As before, linear approximations for the curves of Figs. 7(a) and 7(b) may be made, and circles generated which are defined by

$$\frac{1}{2u_+} = \frac{\omega_M}{2} \frac{\zeta^2(\rho_0^2\omega_H + k_0^2\omega_M)}{\omega_H(\rho_0^2\omega_H + k_0^2\omega_M) + (\omega\zeta)^2} \tag{21a}$$

$$\frac{1}{2v_+} = \frac{\omega_M}{2\omega_R} \frac{\zeta^2(\rho_0^2\omega_H + k_0^2\omega_M)^2}{(\rho_0^2\omega_H + k_0^2\omega_M)^2 - (\omega\rho_0\zeta)^2} \tag{21b}$$

with the assumption $(\omega_R/\omega)^2 \approx 0$.

The circles of constant ω_H will always be centered on the positive real axis. Their maximum radius is $(k_0^2/2)(\omega_M/\omega)^2$ and their minimum radius is zero. This restricted range results in a nearly constant value of ρ^2 with a very small imaginary part since the constant ω_R circle has a very large radius. This corresponds to the ordinary mode behavior.

V. The Points of Maximum Loss and Maximum Phase Shift

From ρ^2, the transverse propagation constant (ρ) is found by taking the negative square root. This choice of sign insures attenuation with increasing transverse coordinate. For example, for a plane electric field

$$E = E_0 \exp[-j(\bar{k}\cdot\bar{R})]$$
$$= E_0 \exp[-j(\rho r \sin\theta + \zeta z \cos\theta)]$$

and with $\rho = \rho' - j|\rho''|$

$$E = E_0 \exp[-|\rho''| r \sin\theta] \exp[-j(\rho' r \sin\theta + \zeta z \cos\theta)]. \tag{22}$$

The maximum value of $|\rho''|$ as a function of applied magnetic field may be found from the construction of Fig. 8(a). Maximum loss occurs at the maximum $|\rho''|$. Since $\rho = \sqrt{c}\, e^{-j(\delta/2)}$ and $\rho'' = -j\sqrt{c} \sin \delta/2$ for maximum ρ'',

$$\frac{d}{d\delta}\left(-j\sqrt{c}\sin\frac{\delta}{2}\right) = 0,$$

or

$$\left(\tan\frac{\delta}{2}\right)\frac{dc}{d\delta} + c = 0. \tag{23a}$$

Using the law of cosines one obtains

$$\frac{dc}{d\phi} = \frac{-ac\sin\phi}{c - a\cos\phi}. \tag{23b}$$

Notice that

$$\delta = \phi + \beta$$

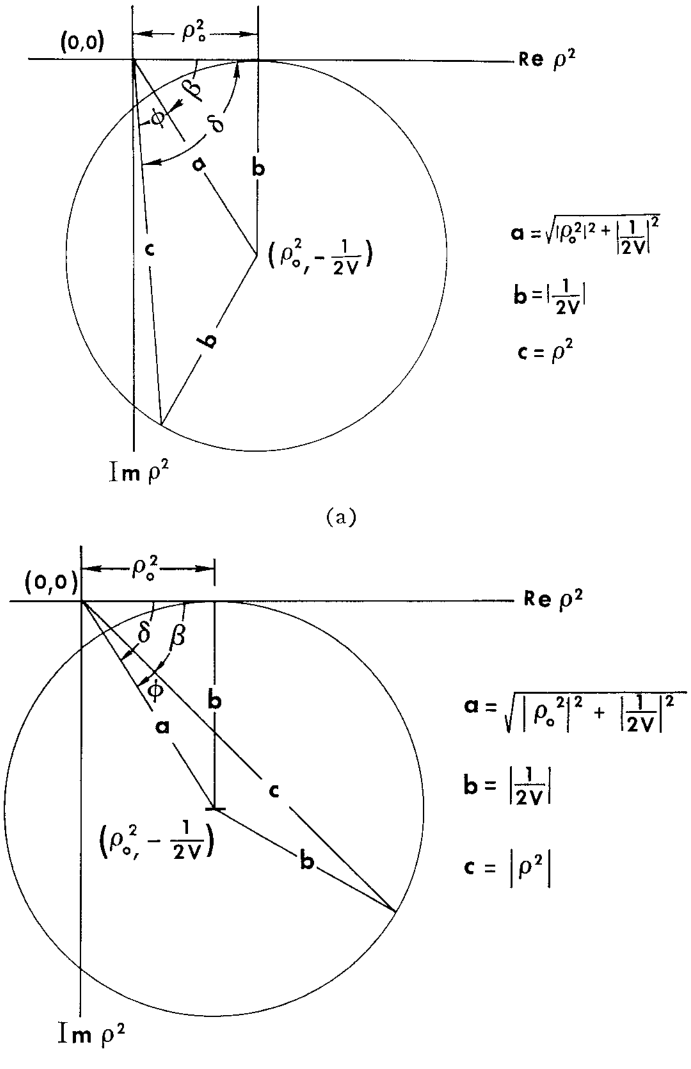

Fig. 8—(a) Construction for maximum loss point. (b) Construction for maximum phase shift point.

and

$$d\delta = d\phi,$$

since β is a constant fixed by the value of ρ_0^2 and the location of the center of the circle. Combining (23a) and (23b) yields the following transcendental equation for the maximum loss point:

$$\frac{c}{a} = \sin\beta\left(\frac{\sin\delta}{1 + \cos\delta}\right) + \cos\beta. \tag{24a}$$

The maximum phase shift point is found from the construction of Fig. 8(b) with the result

$$\frac{c}{a} = \sin\beta\left(\frac{1 + \cos\delta}{\sin\delta}\right) - \cos\beta. \tag{24b}$$

These transcendental equations may be readily solved by applying the constructions of Figs. 8(a) and 8(b),

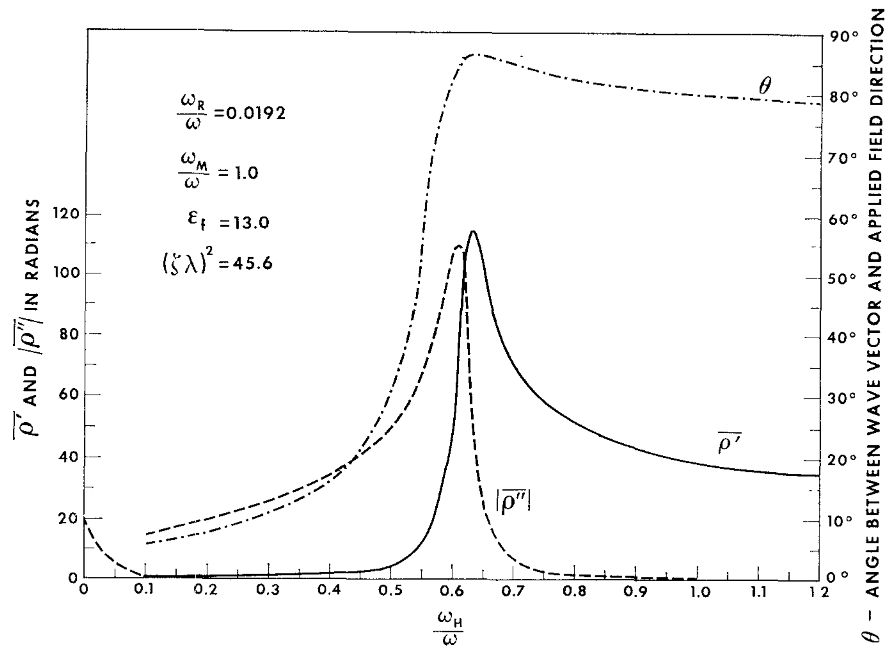

Fig. 9—Real and imaginary parts of normalized transverse propagation constant and wave vector angle as functions of applied magnetic field.

respectively, to the circular locus derived in Section IV. The maximum attenuation occurs at an applied field for which $\omega_H(\rho_0^2\omega_H+k_0^2\omega_M)<(\omega k_0)^2$, while the maximum phase shift occurs for $\omega_H(\rho_0^2\omega_H+k_0^2\omega_M)>(\omega k_0)^2$. For $\omega_H>\omega$, the magnetic losses are essentially zero. The complex propagation constant $\rho=\rho'-j|\rho''|$ is plotted in Fig. 9 for values of ρ^2 taken from Fig. 13. The normalization $\bar{\rho}=(\rho\lambda)$ has been made.

VI. Angles of Wave Vector With Magnetic Field

The two ρ components of the plane wave will propagate through the ferrite at angles dependent upon the applied field, the ferrite parameters and the longitudinal propagation constant. These angles may be computed from Fig. 1,

$$\cos\theta_i = \frac{1}{\sqrt{1+\left(\frac{\rho_i'}{\zeta}\right)^2}}\,. \qquad (25)$$

The behavior of θ_1 is shown in Fig. 9. The angle θ_2 is essentially constant since $(\rho_2')^2$ varies slowly with ω_H/ω. The angle of propagation is a function of the loss parameter ω_R since ρ' depends on it.

VII. Application of Method

Tannenwald and Seavey [1] examine the case of a plane wave normally incident on a semi-infinite ferrite and compute the power absorbed by the ferrite when the applied magnetic field is parallel to the air-ferrite interface. The ratio of the power absorbed to the incident power is shown to be

$$\left|\frac{P}{P_0}\right| = \frac{4\beta_0\epsilon_f\overline{\rho'}}{(\beta_0\epsilon_f)^2+|\rho|^2+2\beta_0\overline{\rho'}\epsilon_f}, \qquad (26a)$$

where $\beta_0=\omega/C$.

When the transverse propagation constant is normalized by the wavelength ($\bar{\rho}=\rho\lambda$), (26a) becomes

$$\left|\frac{P}{P_0}\right| = \frac{8\pi\epsilon_f\overline{\rho'}}{(2\pi\epsilon_f)^2+|\bar{\rho}|^2+4\pi\epsilon_f\overline{\rho'}}\,. \qquad (26b)$$

This expression is easily evaluated as a function of applied field for a specific ferrite by the method described herein.

For the case of transverse propagation

$$\zeta = 0$$
$$k = \rho$$
$$k_0^2 = \rho_0^2,$$

and (7) becomes

$$X^2[\omega_C(\omega_C+\omega_M)-\omega^2] - k_0^2X[\omega_M(\omega_C+\omega_M)] = 0$$

with solutions

$$X = (\rho^2-\rho_0^2) = 0 \quad \text{ordinary mode}$$

$$X = \frac{k_0^2\omega_M(\omega_C+\omega_M)}{\omega_C(\omega_C+\omega_M)-\omega^2} \quad \text{extra-ordinary mode.}$$

The transformation Y now becomes

$$Y = \frac{1}{X} = \frac{1}{k_0^2\omega_M}\left[\omega_C - \frac{\omega^2}{\omega_C+\omega_M}\right],$$

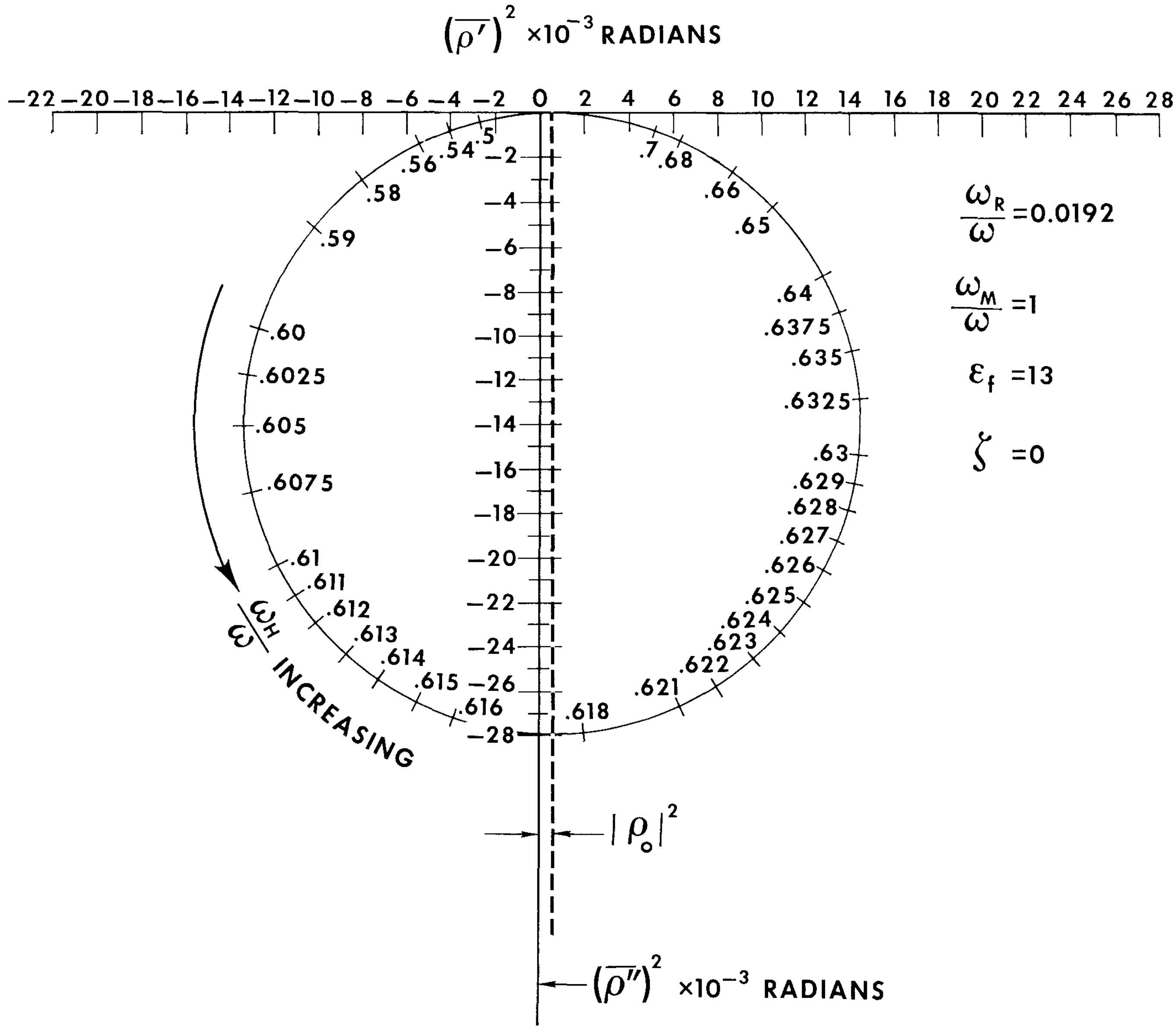

Fig. 10—Circular locus of square of normalized transverse propagation constant as a function of applied magnetic field for case of transverse propagation.

which, assuming that $(\omega_R/\omega)^2 \approx 0$, has real and imaginary parts

$$u = \frac{1}{k_0\omega_M}\left[\omega_H - \frac{\omega^2}{\omega_H + \omega_M}\right]$$

$$v = \frac{\omega_R}{k_0^2\omega_M}\left[1 + \frac{\omega^2}{(\omega_H + \omega_M)^2}\right].$$

An average value for the v coordinate may be again defined as

$$\bar{v} = \frac{\omega_R}{2k_0^2\omega_M}\left\{2 + \omega^2\left[\frac{1}{(\omega_{H_1} + \omega_M)^2} + \frac{1}{(\omega_{H_2} + \omega_M)^2}\right]\right\}.$$

The centers of the constant applied field circles are then given by $[\rho_0^2 + (1/2u), 0]$ and the center of the constant loss circle is $[\rho_0^2, -(1/2\bar{v})]$. The locus of Fig. 10 is obtained for the following parameters

$$\frac{\omega_{H_1}}{\omega} = 0.1 \quad \frac{\omega_M}{\omega} = 1.0 \quad k_0^2 = \left(\frac{\omega}{c}\right)^2 \epsilon_f = 13\left(\frac{\omega}{c}\right)^2$$

$$\frac{\omega_{H_2}}{\omega} = 1.0 \qquad \frac{\omega_R}{\omega} = 0.0192.$$

The magnitude $|\bar{\rho}|^2$ is measured from the origin. The real part of the propagation constant is $\overline{\rho'} = \sqrt{|\bar{\rho}|^2} \cos \psi/2$ where ψ is the angle between the positive real axis and the line from the origin to the value of $|\bar{\rho}|^2$ in question. The real and imaginary parts of $\bar{\rho}$ are shown in Fig. 11, while the absorbed power is shown in Fig. 12 as a function of the applied magnetic field.

When the applied magnetic field is zero, $\rho^2 = \rho_0^2$ $(\rho' = \rho_0)$ and (26b) reduce to

$$\left|\frac{P}{P_0}\right| = \frac{4\sqrt{\epsilon_f}}{\epsilon_f + 1 + 2\sqrt{\epsilon_f}}.$$

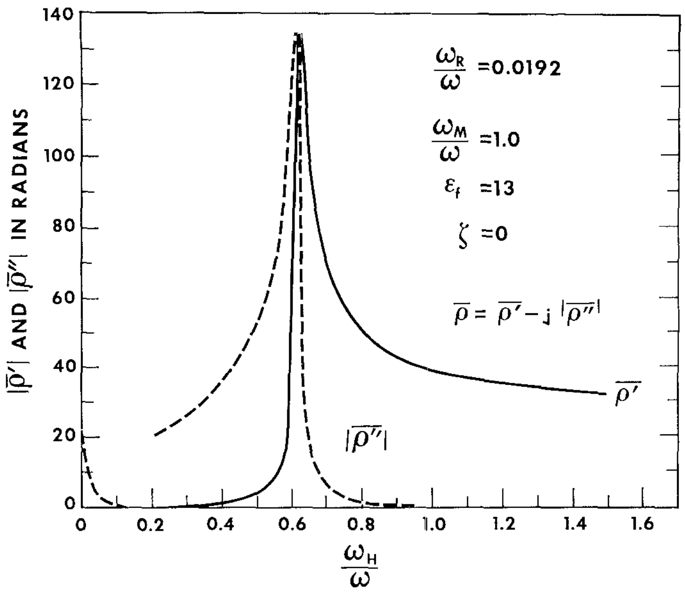

Fig. 11—Real and imaginary parts of normalized transverse propagation constant as a function of applied magnetic field.

VIII. Conclusions

The square of the transverse propagation constant has an approximately circular locus when plotted in the complex plane as a function of applied magnetic field. The radius of this circle is directly proportional to the ferrite saturation magnetization (ω_M), the ferrite dielectric constant (k_0) and is inversely proportional to the longitudinal propagation constant (ζ) and the loss parameter (ω_R). The constant loss circle and the value of the square of the transverse propagation constant for a particular value of applied field are obtained by a graphical technique obviating the need for a digital computer unless extreme accuracy is required.

If no loss is present the ferrite is cut off until $\omega_H(\rho_0{}^2\omega_H + k_0{}^2\omega_M) = k_0{}^2\omega^2$ since for values of ω_H less than this value ρ^2 is real and negative. In a lossy ferrite, propagation is possible for any value of applied field. The angle between the wave vector and the applied magnetic field depends on the loss properties of the ferrite since this determines ρ'.

Appendix

The equation of motion of the ferrite magnetization vector including the Landau-Lifshitz damping term is

$$\frac{d\overline{M}}{dt} = \gamma(\overline{M} \times \overline{H}) - \frac{\alpha\gamma}{|M|}[\overline{M} \times (\overline{M} \times \overline{H})], \qquad (27)$$

where

$\overline{M}$ = the total magnetic field vector including dc and time varying terms
γ = gyromagnetic ratio
$\alpha = \omega_R/\omega = 1/\omega T$ = loss parameter.

By suitable manipulations, expressions for the time varying magnetization components are obtained from

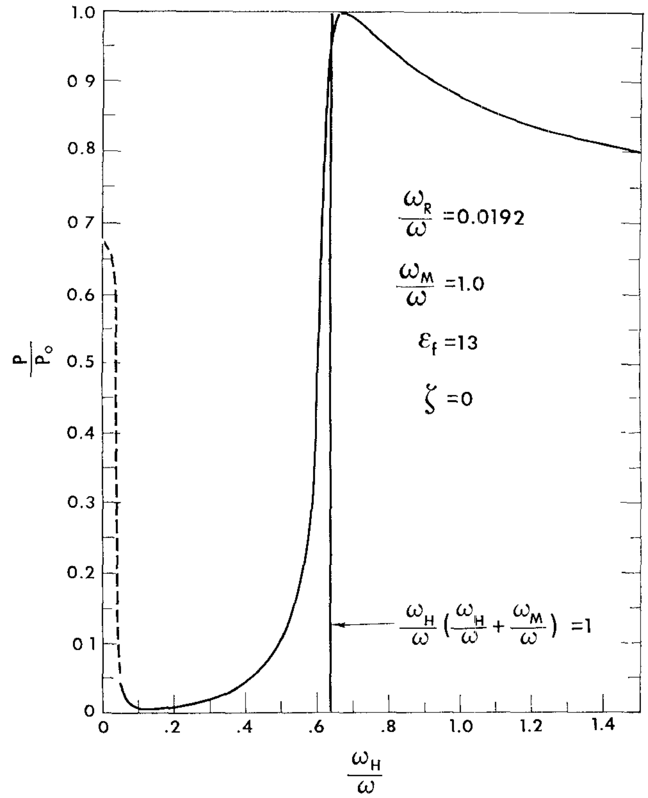

Fig. 12—Ratio of power absorbed to power incident, as a function of applied magnetic field, of a plane wave normally incident on a semi-infinite ferrite which is magnetized parallel to the air-ferrite interface.

which are found the elements of the permeability tensor[6]

$$\mu = 1 + \frac{\omega_M(1+\alpha^2)[\omega_H(1+\alpha^2) + j\omega\alpha]}{[\omega_H(1+\alpha^2) + j\omega\alpha]^2 - \omega^2}$$

$$\kappa = \frac{\omega_M\omega(1+\alpha^2)}{[\omega_H(1+\alpha^2) + j\omega\alpha]^2 - \omega^2}. \qquad (28)$$

If the losses are small $\alpha^2 = (\omega_R/\omega)^2$ may be neglected. Eqs. (28) reduce to

$$\mu = 1 + \frac{\omega_M[\omega_H + j\omega\alpha]}{[\omega_H + j\omega\alpha]^2 - \omega^2}$$

$$\kappa = \frac{\omega_M\omega}{[\omega_H + j\omega\alpha]^2 - \omega^2}. \qquad (29)$$

With the definition $\omega_C = \omega_H + j\omega_R$, these reduce to the form of (2) and (3).

To obtain an exact solution for the square of the transverse propagation constant (5) may be solved directly. When expanded in terms of the ferrite parameters (30) results:

[6] See Lax and Button [8], p. 152.

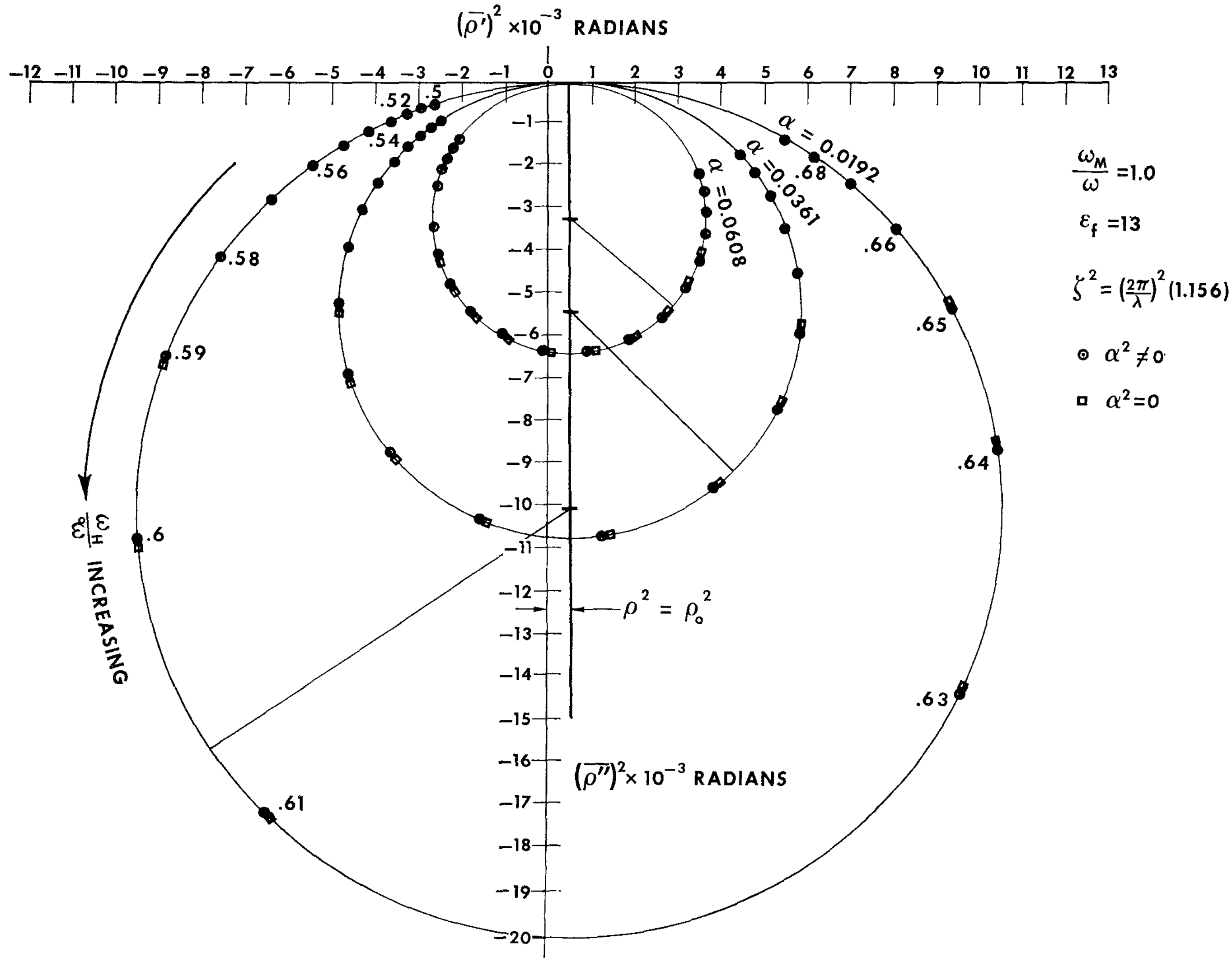

Fig. 13—Computed circular locus of square of normalized transverse propagation constant as function of applied magnetic field for several values of the loss parameter showing effect of approximation $(\omega_R/\omega)^2=0$.

$$
\begin{aligned}
\rho^2 = \frac{1}{2}\cdot\frac{1}{\omega_H(\omega_H+\omega_M)(1+\alpha^2)+j\omega_R(2\omega_H+\omega_M)-\omega^2}
&\cdot\Big\{\rho_0{}^2\big[\omega_H(2\omega_H+\omega_M)(1+\alpha^2)-2\omega^2+j\omega_R(4\omega_H+\omega_M)\big]+\omega_M k_0{}^2\big[(1+\alpha^2)(2\omega_H+\omega_M)+j\omega_R\big] \\
&\pm\,\omega_M\sqrt{\big[\rho_0{}^2(\omega_H+j\omega_R)+\rho_0{}^2\alpha^2\omega_H+k_0{}^2\omega_M(1+\alpha^2)\big]^2+(2\omega k_0\zeta)^2}\Big\}.
\end{aligned}
\qquad (30)
$$

Digital computer values for $(\bar{\rho})^2=(\rho\lambda)^2$ were obtained from (30) for $(\omega_R/\omega)^2=\alpha^2\neq 0$ and for $\alpha^2=0$. Fig. 13 shows the effect of the approximation for certain typical ferrites.

Acknowledgment

The author would like to thank G. A. Deschamps of the University of Illinois for his comments concerning this paper and for the fruitful discussions which contributed to the successful conclusion of this work.

References

[1] M. H. Seavey and P. E. Tannenwald, "Electromagnetic Propagation Effects in Ferromagnetic Resonance," M.I.T. Lincoln Lab., Lexington, Mass., Tech. Rept. No. 143; 1957.
[2] F. J. Rosenbaum and P. D. Coleman, "Cerenkov radiation in anisotropic ferrites," IRE Trans. on Microwave Theory and Techniques, vol. MTT-11, pp. 302–311; September, 1963.
[3] P. H. Smith, "Transmission-line calculator," *Electronics*, vol. 12, pp. 21–31; January, 1939.
[4] D. Polder, "On the theory of ferromagnetic resonance," *Phil. Mag.*, vol. 40, pp. 99–115; 1949.
[5] G. A. Deschamps and W. L. Weeks, "Charts for computing the refractive indexes of a magneto-ionic medium," IRE Trans. on Antennas and Propagation, vol. AP-10, pp. 305–317; May, 1962.
[6] S. Sensiper, "Resonance loss properties of ferrites in the 9 kMc region," Proc. IRE, vol. 44, pp. 1323–1342; October, 1956.
[7] R. E. Churchill, "Introduction to Complex Variables and Applications," McGraw-Hill Book Co., Inc., New York, N. Y., pp. 54–55; 1948.
[8] B. Lax and K. J. Button, "Microwave Ferrites and Ferrimagnetics," McGraw-Hill Book Co., Inc., New York, N. Y.; 1962.
[9] M. L. Kales, "Modes in wave guides containing ferrites," *J. Appl. Phys.*, vol. 24, pp. 604–608; May, 1953.